Nuclear Instruments and Methods in Physics Research A280 (1989) 564–567
North-Holland, Amsterdam

DIFFUSION ENHANCEMENT IN Fe–Ni ALLOYS DURING FAST-NEUTRON IRRADIATION

V. SCIANI and G. LUCKI

Radiation Damage Division of IPEN-CNEN/SP, CP 11048, 05508 Pinheiros, São Paulo, Brazil

The effect of fast-neutron irradiation on Fe–Ni (50–50 at.%) alloys has been analyzed at high temperatures by means of the magnetic after-effect. At $T \lesssim T_m/2$ (T_m = melting point) there existed enhanced diffusion conditions, due to neutron-produced vacancies with an activation energy of 1.41 eV. At $T \gtrsim T_m/2$, the diffusion is described by a thermal effect with an activation energy of 3.06 eV, becoming independent of the irradiation. Results of an Fe–Ni alloy doped with 0.1 at.% Cr and 50 ppm Mo are also presented.

1. Introduction

The search for radiation-damage-resistant materials is important for the development of nuclear technology. In this framework, irradiation-produced diffusion enhancement is of special interest for the understanding of the mobility of point defects and their agglomerates and consequently the changes in micro- and macroscopic physical properties, such as swelling.

A relation between the partial diffusion coefficient in alloys and the magnitude of swelling under irradiation has been proposed by Venkler and Ehrlich [1] for the case where the partial diffusion coefficients of the components of an alloy differ some orders of magnitude in the temperature range where swelling occurs: the slowly diffusing atoms prevent void formation due to their relative immobility while the vacancies change lattice positions with the fast substitutional component and migrate to other sinks. The segregation in irradiated alloys was considered by Marwick [2], where the theory of the Kirkendall effect was extended to include the effects of vacancy gradients in binary alloys in order to apply in irradiated metals: one consequence of segregation is the induction of an extra vacancy flux which opposes the radiation-induced vacancy flux to the sink. Probably there is a correlation between the swelling and the diffusion behaviour. The results obtained by Rothman et al. [3] appear to contradict the above-mentioned statement: the diffusion behaviour of the major constituents does not differ between high- and low-swelling alloys. They found no correlation between the swelling and diffusion behaviour of major components.

The main subject of this work is to give a contribution of the study of diffusion on important technological alloys submitted to neutron irradiation. The neutron-irradiation-enhanced diffusion in Fe–Ni alloys by means of the magnetic after-effect method during isothermal annealing out- and inside the IEA-R1 reactor core was emphasized.

0168-9002/89/$03.50

2. Experimental details

The Fe–Ni system studied had compositions near 50–50 at.%. The temperature range explored was limited by two critical phenomena: the Curie point (780 K) and the order–disorder transformation temperature (590 K). In this range the system is face centered cubic.

The samples were of toroidal shape, 0.4 mm thick, having an external diameter of 17.4 mm and an internal one of 11 mm. They were fabricated from Johnson Mathey zone-refined ingots, with the following nominal compositions and initial thermal treatments:

(a) Fe–Ni (50–50 at.%): annealed at 1173 K during 1 h;
(b) Fe–Ni–Mo (50–50 at.% + 50 ppm): annealed at 1073 K during 1 h; and
(c) Fe–Ni–Cr (49.95–49.95–0.1 at.%): annealed at 1123 K during 15 h.

All samples were annealed in hydrogen and slowly cooled inside the furnace.

The initial magnetic permeability from samples with primary and secondary windings was followed by a lock-in amplifier during isothermal annealings between 673 and 773 K out- and inside the core of the IEA-R1 swimming-pool reactor of the Instituto de Pesquisas Energéticas e Nucleares in São Paulo, Brazil, with an instant flux of 5×10^{12} n/(cm^2 s). All annealing was performed in an argon atmosphere.

The experimental technique used is called the magnetic after-effect [4,5] which allows an evaluation of the time constants and activation energies from the experimental curves of initial permeability disaccommodation. The time constants were calculated by means of the Brissonneau method [6].

The mechanism which permits the detection of the defect movements is the establishment of short-range order. It was supposed [4] that the migration of defects permits the reorientation of atom pairs (e.g. Fe–Ni,

Ni–Ni or Fe–Fe). The spontaneous magnetization commands this reorientation and progressively establishes the short-range order which tends to materialize the geometry of the internal magnetic anisotropy. After demagnetization, during the relaxation process at a given temperature, the Bloch walls are agitated by a weak (~ 1 mOe) and alternating (35 Hz) magnetic field. As a consequence of this, a progressive immobilization of Bloch walls occurs, allowing the detection of an exponential decrease of the initial magnetic permeability.

The directional short-range order, once established during an isothermal annealing, must be completely destroyed before a subsequent annealing is made at a given temperature to have reproducible experiments. Therefore the sample treatment for each isothermal annealing obeyed the following sequence:

(a) the sample was thermally demagnetized above the Curie point;
(b) a demagnetization alternating magnetic field (~ 30 Oe) was applied until the sample had attained the preestablished annealing temperature, thus assuring the maintenance of the disordered state, and
(c) the annealing temperature once established, the sample was demagnetized and a weak (~ 1 mOe) and alternating (35 Hz) magnetic field was applied which allowed a reversible displacement of the Bloch walls (Rayleigh region) and the measurement of the corresponding disaccommodation process.

The experimental apparatus was a classical set for magnetic after-effect measurements, basically consisting of a lock-in amplifier, temperature regulator and an annealing furnace with controlled atmosphere. Details of this apparatus have been described earlier [7].

3. Results and discussion

Fig. 1 and 2 show the initial magnetic permeability disaccommodation curves for several temperatures for

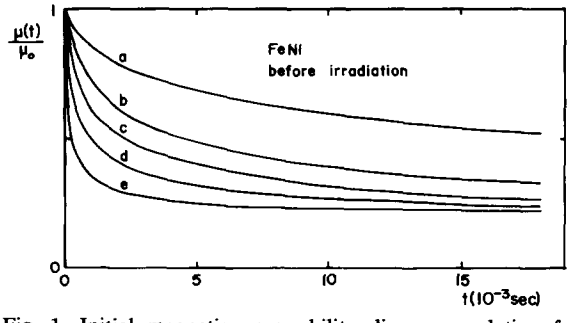

Fig. 1. Initial magnetic permeability disaccommodation for Fe–Ni before irradiation at (a) 400 °C, (b) 420 °C, (c) 440 °C, (d) 460 °C and (e) 480 °C.

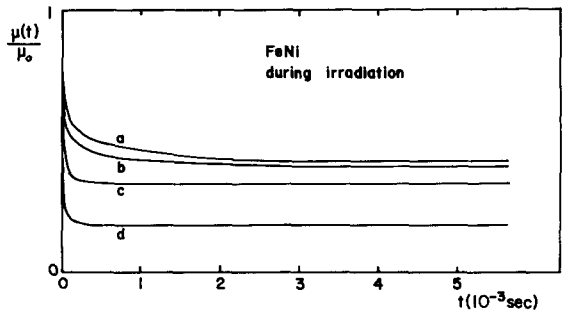

Fig. 2. Initial magnetic permeability disaccomodation for Fe–Ni during irradiation at (a) 420 °C, (b) 440 °C, (c) 460 °C and (d) 480 °C.

Fe–Ni, before and during irradiation respectively. Similar curves for Fe–Ni–Cr and Fe–Ni–Mo can be seen in ref. [7].

The initial magnetic permeability obeys the following phenomenological law [4,6]:

$$\frac{\frac{1}{\mu(t)}-\frac{1}{\mu_0}}{\frac{1}{\mu_\infty}-\frac{1}{\mu_0}}=1-\exp\left(-\frac{t}{\tau}\right), \tag{1}$$

where $\mu(t)$ is the initial permeability for a time t, μ_0 the initial value of $\mu(t)$, for $t=0$, μ_∞ the final value of $\mu(t)$, for $t=\infty$, and τ the time constant of the disaccommodation process. It was assumed that the time constant can be expressed by an Arrhenius law:

$$\tau=\tau_\infty \exp\left(\frac{E}{kT}\right), \tag{2}$$

where τ_∞ is the time constant at infinite temperature, E the activation energy for the reorientation process, k the Boltzmann constant and T the absolute temperature. The time constants are derived as a function of temperature from the initial magnetic disaccommodation curves by applying eq. (1) and plotted in fig. 3 as a function of the reciprocal temperature, according to eq. (2).

The activation energies for unirradiated (E_{Th}: before irradiation) and irradiated (E_{irr}: during irradiation) samples, obtained from fig. 3 by applying eq. (2), are given in table 1. These results agree with those obtained by Veissid et al. [8] in the same alloys and temperature range. An activation energy of $E_{Th}=3.34$ eV was determined by means of magnetic anisotropy energy for unirradiated Fe–Ni, and of $E_{irr}=1.34$ eV during irradiation by magnetic after-effect method, in the Melousine Reactor in Grenoble [9], giving results comparable with those presented in this article. Gerstner and Kneller [10] found an activation energy of 2.64 eV for the diffusion of Fe–Ni (40–60 at.%) and Rothman et al. [3] found an activation energy of 3.1 eV for the diffusion of Fe, Ni

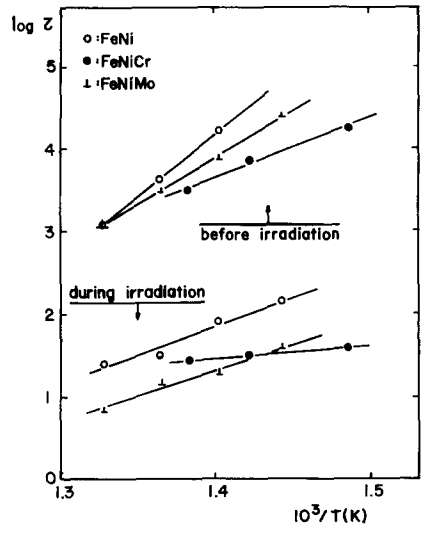

Fig. 3. Time constants derived from the initial magnetic disaccomodation curves as a function of reciprocal temperature for Fe–Ni, Fe–Ni–Mo and Fe–Ni–Cr.

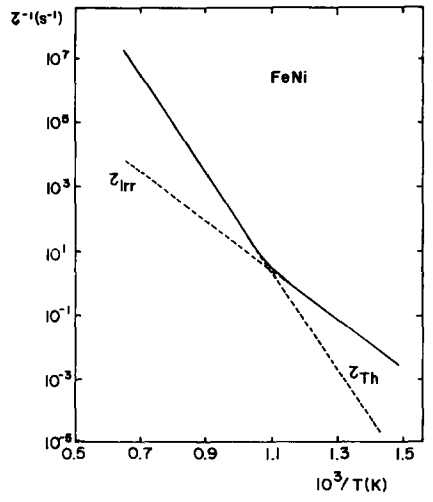

Fig. 4. Reciprocal of the time constant as a function of the reciprocal of the temperature for Fe–Ni.

and Cr in Fe–Ni–Cr alloys on nonirradiated specimens. Self-diffusion data for pure metals can be seen in ref. [11]: the self-diffusion energy in nickel is 2.88 eV and in γ-iron it is 2.95 eV. Thus the value of $E_{Th} = 3.06$ eV for Fe–Ni seems reasonable. From table 1 it can be seen that the addition of impurities decreases the activation energy: the addition of 50 ppm of Mo lowers it to 2.88 eV and that of 0.1 at.% of Cr to 1.45 eV.

It is known that neutron irradiation produces foreign elements by transmutation reactions which can cause changes of the chemical composition and may induce phase instabilities or precipitations. In this work this effect is negligible: a fluence of 10^{18} n/cm^2 produces a maximum impurity concentration of 2 ppm in Fe–Ni (50–50 at.%) [12].

Figs. 1, 2 and 3 clearly show, in the measured temperature range, the enhancement of diffusion induced by fast-neutron irradiation during isothermal annealings. To allow a better view of this enhancement of diffusion, we can extrapolate the experimental data to higher temperatures. Fig. 4 shows the reciprocal of the time constant as a function of reciprocal temperature for Fe–Ni. Here it can be supposed that the measurements were performed in steady state so that the diffusion coefficient, D_{eff}, is proportional to τ^{-1}.

Table 1
Activation energies evaluated from fig. 3 by applying eq. (2)

Sample	E_{Th} [eV]	E_{irr} [eV]
Fe–Ni	3.06 ± 0.21	1.41 ± 0.10
Fe–Ni–Mo	2.30 ± 0.16	1.25 ± 0.09
Fe–Ni–Cr	1.45 ± 0.11	0.30 ± 0.02

At high temperatures, $T \gtrsim T_m/2$ ($T_m = 1710$ K is the melting point), the thermal-vacancy creation is large compared to the production of vacancies by irradiation because in this temperature range the defect mobilities are high so that the irradiation-induced defects are lost quickly [13]. In this case the diffusion is not affected by irradiation, i.e. the diffusion becomes independent of the irradiation and has an activation energy of $E_f^v + E_m^v$, the sum of the energies of vacancy formation and migration respectively [13,14], and corresponds to the extrapolation at high temperatures ($T \gtrsim T_m/2$) of the experimental data obtained before irradiation (the heavy line in fig. 4 at $T \gtrsim T_m/2$) with $E_{Th} = 3.06$ eV.

At temperatures $T \lesssim T_m/2$ the reciprocal of the time constant during irradiation, τ_{irr}^{-1}, becomes much larger than τ_{Th}^{-1} and the activation energy drops to 1.41 eV. This means that the concentration of irradiation-produced vacancies becomes higher than that of thermal-equilibrium vacancies. For example, at 700 K for Fe–Ni, $\tau_{irr}^{-1} = 8.4 \times 10^{-3}$ s^{-1}. This represents a great enhancement (a factor 350) compared to the thermal effects with $\tau_{Th}^{-1} = 2.4 \times 10^{-5}$ s^{-1}. In this temperature range there exists a vacancy concentration above the thermal equilibrium value, i.e. a vacancy supersaturation. As τ^{-1} is proportional to the vacancy concentration, C^v, the vacancy supersaturation, S_v, can be expressed as:

$$S_v = \frac{C_{irr}^v}{C_{Th}^v} = \frac{\tau_{Th}^{-1}}{\tau_{irr}^{-1}}. \tag{3}$$

Plotted in fig. 5 is the supersaturation of vacancies, S_v, derived from fig. 3 by applying eq. (3), as a function of temperature. Notice a decrease in the values of the vacancy supersaturation with increasing temperature, which tends to unity at $T \approx T_m/2$, that is, the irradia-

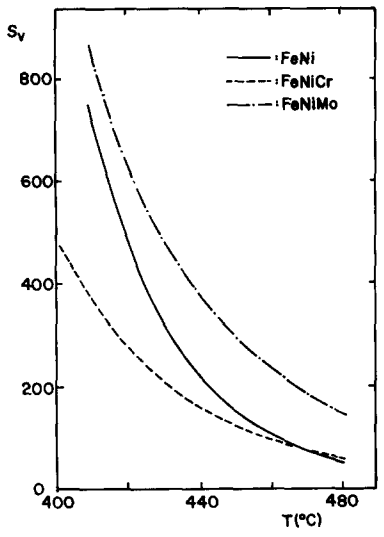

Fig. 5. Supersaturation of vacancies as a function of temperature for Fe–Ni, Fe–Ni–Mo and Fe–Ni–Cr.

tion-produced vacancies tend to the thermal values, causing a decrease in the supersaturation values. This fact can be seen clearly in fig. 4: at a temperature $T_m/2$ and above, the irradiation effect is negligible compared to the thermal effect.

From fig. 5 it can be seen that the effect of Cr and Mo as impurities is antagonistic to the vacancy supersaturation. The Cr atoms have the effect of stabilizing the vacancy supersaturation between 400 and 470 ° C. It was found [8] that a sample doped with 2 at.% of Si has a supersaturation about 100 times smaller than pure Fe–Ni at 450 ° C. Thus, the heavy line in fig. 5 means a measurement of a diffusion during irradiation and can

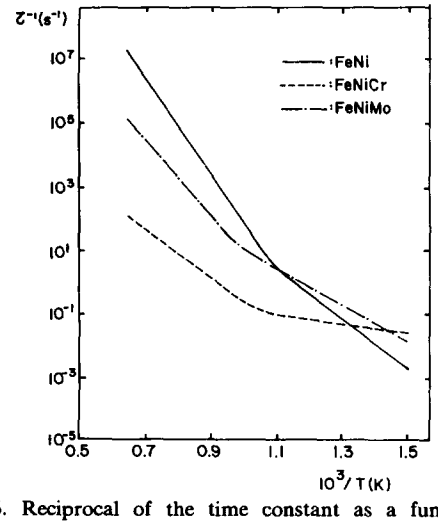

Fig. 6. Reciprocal of the time constant as a function of reciprocal temperature for Fe–Ni, Fe–Ni–Mo and Fe–Ni–Cr.

be separated into two temperature ranges: at high temperature only the thermal effects predominate and below $T_m/2$ the diffusion enhanced by neutron irradiation.

Fig. 6 shows the reciprocal of the time constant as a function of the reciprocal temperature for Fe–Ni, Fe–Ni–Cr and Fe–Ni–Mo. The figure shows that at temperatures $\lesssim T_m/2$ the diffusion is enhanced due to irradiation, for the three alloys studied, with an activation energy of 1.25 and 0.30 eV for Fe–Ni–Mo and Fe–Ni–Cr respectively. At temperatures above $T_m/2$ the thermal effects predominate and the activation energies go to 2.30 eV for Fe–Ni–Mo and 1.45 eV for Fe–Ni–Cr.

4. Conclusions

The effect of neutron irradiation on diffusion in Fe–Ni alloys has been investigated by means of the magnetic after-effect method. For temperatures $T \lesssim T_m/2$, the diffusion is enhanced by fast-neutron-irradiation-produced vacancies. In this temperature range the vacancy supersaturation values have been calculated and tend to unity at $T \simeq T_m/2$. It was found that the effect of Cr and Mo as impurities is antagonistic to the vacancy supersaturation and the Cr atoms have the effect of stabilizing the supersaturation between 400 and 470 ° C. For $T \gtrsim T_m/2$, the diffusion is described by the thermal effect, becoming independent of irradiation.

References

[1] H. Venkler and K. Ehklich, J. Nucl. Mater. 60 (1976) 347.
[2] A.D. Marvick, J. Phys. F8 (1978) 1849.
[3] S.J. Rothman, L.J. Novicki and G.E. Murch, J. Phys. F10 (1980) 383.
[4] L. Néel, J. Phys. Rad. 13 (1952) 249.
[5] P. Moser, Doctor Thesis, University of Grenoble, Grenoble, France (1965).
[6] P. Brissonneau, J. Phys. Chem. Solids 7 (1958) 22.
[7] V. Sciani, M. Sc. Thesis, IPEN-CNEN/SP, Brazil (1978).
[8] N. Veissid, S. Watanabe and G. Lucki, J. Nucl. Sci. Technol. 21 (1984) 215.
[9] G. Lucki, W. Chambron, J. Verdonne and S. Watanabe, Proc. 4th Int. Conf. on Materials Technology, Caracas, Venezuela, 1975 (Regional Technical Aid Center, Mexico, 1975) p. 271.
[10] P. Gerstner and E. Kneller, J. Appl. Phys. 32 (9161) 364S.
[11] N.L. Peterson, J. Nucl. Mater. 69/70 (1978) 3.
[12] N. Veissid and G. Lucki, Proc. 3rd Brazilian Conf. on Engineering and Materials Science, Rio de Janeiro, Brazil, 1978 (COPPE/Federal University of Rio de Janeiro, Brazil, 1978) p. M5.1.
[13] H.J. Frost and K.C. Russel, in: Phase Transformation During Irradiation, ed. F.V. Nolfi, Jr. (Applied Science Publishers, 1983) p. 75.
[14] S.J. Rothman, ibid., p. 189.